Journal of Trace Elements in Medicine and Biology 52 (2019) 58–67

Contents lists available at ScienceDirect

Journal of Trace Elements in Medicine and Biology

journal homepage: www.elsevier.com/locate/jtemb

Pathobiochemistry

Suppression of proliferation and activation of cell death by sodium selenite involves mitochondria and lysosomes in chemoresistant bladder cancer cells

K. Soukupová, E. Rudolf*

Department of Medical Biology and Genetics Charles University, Faculty of Medicine in Hradec Králové, Zborovská 2089, 500 03 Hradec Králové, Czech Republic

ARTICLE INFO

Keywords:
Bladder cancer
Selenite
Mitochondria
Lysosomes
Autophagic cell death
Necrosis

ABSTRACT

The specific effects of sodium selenite (selenite) on a chemoresistant human bladder cancer cell line RT-112/D21 were investigated during 72 h. Selenite at low concentration of 2.5 µmol (otherwise tolerated in normal urothelial cells UROtsa) suppressed growth and proliferation of the tested cancer cells via induced oxidative stress. Selenite further altered mitochondrial functions (i.e. decreased mitochondrial membrane potential, increased production of superoxide and reduced ATP synthesis), disrupted lysosomal membranes and activated autophagy. These changes in selenite-exposed cells ultimately resulted in their demise via necrosis and other cell death modality displaying heterotypic apoptotic and autophagic features.

1. Introduction

Physiological and life-supporting roles of selenium in eukaryotic organisms have long been recognized. Selenium is known to strongly influence a number of biochemical and molecular processes in individual cells as well as tissues including synthesis of proteins, regulation of redox and stress signaling in addition to mediating immunomodulatory and metabolic activities [1]. Selenium is thus considered an important trace element in animals including human beings and any disturbances in selenium intake result in an increased susceptibility to a range of pathologies and diseases [2]. Accordingly, numerous experimental and epidemiologic studies brought evidence concerning the relationship between selenium levels and cancer risks in humans [3].

Cancer of urinary bladder belongs among relatively common malignancies in developed countries where majority of all incident cases are diagnosed. The most common risk factor is tobacco use, namely cigarette smoking, which may account for about half of male urinary tract malignancies and up to one-third of female urinary track cancers. Other risk factors might include male sex, infection, diet and occupational exposures, particularly to aromatic amines and polycyclic aromatic hydrocarbons (PAH), although their contributions to the development of this malignancy seem to be limited and not entirely clear [4]. Most bladder cancers are at the time of diagnosis non-muscle invasive which frequently recur but do not often invade and metastasize while muscle-invasive malignancies present less favorable prognosis due to metastasizing [5]. Despite the fact that our understanding of molecular features and heterogeneity of bladder cancer improved significantly over the past decades, treatment has not advanced correspondingly and new approaches to systemic therapy and/or prevention are needed [6]. One potentially beneficial preventive factor in this respect is selenium, in particular its inorganic form selenite. [7].

Both existing organic and inorganic selenium forms display often opposite extracellular and intracellular chemistries which to the large degree determine their final biological effects in target cancer cells. These range from supportive and pro-survival roles mediated for instance by synthesized selenoproteins [8] to metabolically produced hydrogen selenide and its dependent oxidative stress, macromolecular damage and stress signaling leading to cellular injury and ultimate cell death. In this respect it is especially inorganic selenite which has been intensively studied as an inhibitory agent in a number of malignancy models [3,9,10] due to its rather strong toxic effects which, in addition, seem to be selective for tumor cells only [11].

Most selenite-dependent effects are attributed to increased levels of ROS that are known to arise from selenite intracellular metabolism [12]. Available evidence concerning selenite-dependent effects in malignant cells further shows that this element targets many intracellular molecules and processes and may induce several cell death modalities [13–15]. Many if not all malignant tumors develop chemoresistance via dysregulation or suppression of the main pro-death signaling, mainly apoptotic [16,17]. Thus selenite by its multi-faceted activity may overcome such apoptotic resistance via alternative routes and that is why it is important to investigate its effects in detail [18,19]. In particular, in malignancies where our mechanistical knowledge over their

* Corresponding author.
E-mail address: rudolf@lfhk.cuni.cz (E. Rudolf).

https://doi.org/10.1016/j.jtemb.2018.11.009
Received 20 June 2018; Received in revised form 30 October 2018; Accepted 26 November 2018

selenite sensitivity is still lacking and which present potentially convenient targets for selenite due to its fate in the human body.

In this study we sought to (1) explore the cytotoxic effects of selenite on a chemoresistant human bladder cancer cell line RT-112/D21 as compared to normal human urothelial cells UROtsa. Our next goal was to (2) investigate mechanisms of selenite toxicity in the mentioned cancer cells focusing on select mechanisms and targets such as mitochondria and lysosomes and to (3) analyze the phenotype of ensuing cell death.

2. Materials and methods

2.1. Chemicals

Sodium selenite (Na_2SeO_4 -selenite, anhydrous, Cat. No. S1382), N-acetylcystein (NAC), dimethylsulfoxide (DMSO); 4´, 6-diamidino-2-phenylindole (DAPI), Triton-X; agarose; propidium iodide (PI), ethidium bromide; monodansylcadaverine (MDC), cyclosporin A, acridine orange (AO), Neutral red (NR), 3-methyladenine (3-MA) and pepstatin A were purchased from Sigma-Aldrich (Prague, Czech Republic). JC-1 (5,5′,6,6′-tetrachloro-1,1′,3,3′ tetraethylbenzimidazolylcarbocyanine iodide), MitoSOX™ Red and MitoTracker Green FM were from Life-Technologies Czech Republic (Prague, Czech Republic). Caspase-3 specific inhibitor z-DEVD-fmk, caspase-3-specific substrate (DEVD-AFC) and pan caspase inhibitor z-VAD were from Calbiochem (La Jolla, CA, USA). LC3B, p62, BECLIN-1 as well as AKT and p-AKT were obtained from Cell Signaling Technology, Inc. (Danvers, MA, USA). All other chemicals were in analytical grade.

2.2. Cell lines and treatments

Multidrug resistant human bladder cancer cell line RT112/D21 was provided from Dr. J. Hatina Department of Biology, Faculty of Medicine in Pilsen, Charles University, Czech Republic). This cell line was established by continuous exposure of the parental line RT-112 to increasing concentrations of doxorubicin over a period of 9 months, with resulting manifold higher resistance to doxorubicin and cross resistance to epirubicin and vinblastine [20]. Histologically, the cells are considered as moderately differentiated with intermediate grade due to the original evaluation of the transitional cell carcinoma (histological grade G2) from which parental line RT-112 was established. Immortalized human urothelial cell line UROtsa was a kind gift from prof. Fabarius University Medical Centre Mannheim, University Heidelberg, Germany. Both cell lines were cultivated in RPMI medium (RPMI, Gibco, Prague, Czech Republic) with added 10% fetal calf serum (FCS) (Gibco, Prague, Czech Republic). Cells were kept in an incubator at 37 °C in a humidified atmosphere with 5% CO_2. All experiments were carried out at low passages of both cell lines.

Sodium selenite was dissolved in full treatment medium. The working concentrations were prepared *ad hoc* prior to each individual experiment. The stock solutions of other used chemicals (inhibitors or modulators) were prepared in DMSO or serum-free medium at 1,000 × concentration and stored at 4 °C in the dark. The particular working concentrations of individual chemicals and the time-frame of their use are indicated below:

3-MA (added to cells 30 min prior to selenite exposure at 5 mmol concentration), NAC – (added to cells 24 h prior to selenite exposure at 500 μmol concentration), z-VAD (added to cells simultaneously with selenite at 50 μmol concentration), pepstatin A (added to cells 1 h prior to selenite exposure at 20 μmol concentration) and cyclosporin A (added to cells 30 min prior to selenite exposure at 5 μmol concentration).

2.3. Cytotoxicity assays

Cytotoxicity of selenite in bladder cancer cells RT-112/D21 and urothelial cells UROtsa was measured using Brilliant Blue and Neutral red assays. In both assays cells were seeded (cancer cells at the density of 3×10^4 cells/ml and urothelial cells 2×10^4 cells/ml), grown and exposed to 2.5–10 μmol selenite in 96-well microtiter plates for up to 72 h upon standard cultivation conditions in an incubator at oxygen tensions close to atmospheric (~20%), with the partial pressure of O_2 being roughly 150 mm Hg. In case of Brilliant Blue assay, cells at the particular time interval were washed twice with PBS, fixed with methanol and fixation solution (50% ethanol, 49% H_2O, 1% glacial acetic acid) and stained Brilliant Blue stain solution (0.4 mg/ml). After 1 h incubation at room temperature (RT) the formed blue product was dissolved in potassium acetate ethanol solution and the absorbance was recorded at 450/ 650 nm wavelength. In case of Neutral red assay, cells at the particular time interval were incubated in an incubator with 100 l of NR (80 μg/ml) in fresh medium for 3 h. Next, the medium was removed and 100 l of fixative solution (calcium chloride in 0.5% formaldehyde) was added for 15 min at RT. After two subsequent rounds of washing, cells were lysed with 200 l of lysis solution (1% acetic acid in 50% ethanol) and further incubated for 30 min at RT. The presence of coloured product was measured at 540/620 nm of wavelength.

2.4. Time-lapse analysis of cell morphology

About 25% confluent RT112/D21 and UROtsa cells in plastic tissue-culture dishes with glass bottom were exposed to 2.5–10 μmol selenite in the growth medium for up to 72 h. During entire experiment cells in the tissue-culture dishes were placed and observed in a time-lapse imaging system BioStation IM (Nikon, Prague, Czech Republic) which insures the standard cultivation conditions and allows automatic recording of cellular morphology and behavior. Recording was carried out in a both multipoint and multichannel time-lapse modes and upon a range of magnifications. Obtained sequences were next software (NIS Elements AR 3.20 (Nikon, Prague, Czech Republic)) processed and analyzed with selection of typical frames depicting morphology of individual cells at the particular time intervals.

2.5. Cell proliferation signaling

Selenite (2.5 μmol)-treated RT-112/D21 cancer and UROtsa urothelial cells grown in 96-well microtiter plates with black bottom were at individual time intervals (24 and 48 h) rinsed in PBS, fixed in 4% paraformaldehyde and permeabilized with blocking buffer (PBS with 0.3% Triton-X and 5% BSA). Following the blocking The cells were then incubated with primary antibodies (anti-AKT1 1:100; anti-pAKT1(Ser473) 1:100; anti-AKT2 1:100; anti-pAKT2(Ser474) 1:100, anti-AKT3 1:100; anti-pAKT3(Ser474) 1:100; anti-CYCD 1:100; anti-c-MYC 1:100; anti-ERK1/2 1:100; anti-p38 1:50; anti-TP53 1:100; anti-p21 1:100; anti-p16 1:50, anti-PTEN 1:50 - PathScan® Intracellular Signaling Array Kit, Cell Signaling Technology, Inc. (Danvers, MA, USA) at 4 °C for 24 h. Next day, cells were washed with cold PBS (5 min, RT) three times and secondary antibodies (Alexa Fluor 488 anti-mouse or anti-rabbit (1:250)) were added for 1 h at RT. After washing with PBS, cells were counterstained with DAPI and the fluorescence was analyzed by high-throughput cell scoring system with Cell scoring module of MetaXpress® Image Acquisition and Analysis Software.

2.6. DNA damage

DNA damage in 2.5 μmol selenite-exposed bladder cancer cells during 48 h was measured by the alkali single-cell gel electrophoresis (comet assay). Harvested cells by trypsinization were pelleted by centrifugation (5 min at 1500 rpm and 4 °C - (JOUAN MR 22, Trigon, Prague, Czech Republic)), and embedded in 0.6% agarose on microscopic slides. After cell lysis (lysis buffer - 2.5 M NaCl, 100 mM EDTA, 10 mM Trizma, 1% Triton X-100 and 10% DMSO) for 1.5 h at 4 °C, the electrophoresis in the alkaline buffer (NaOH, EDTA) was carried out at

25 V (300 mA) for 30 min at 4 °C after a 40-min period of unwinding. Slides were next neutralized, drained and cells stained with ethidium bromide. One hundred cells from three independent samples were scored for tail migration intensity (% of DNA in tail) using the double staining LUCIA Comet Assay analysis system LIM (Laboratory Imaging Ltd., Prague, Czech Republic).

2.7. Mitochondrial superoxide production

Mitochondrial superoxide levels in 2.5 μmol selenite exposed chemoresistant bladder cancer cells during 48 h were determined using fluorescent detection of MitoSOX™ Red reagent. Briefly, selenite-exposed and control cells grown in cytospin chambers were co-incubated with MitoSOX™ Red solution (5 μM, 20 min, 37 °C) and MitoTracker Green FM solution (100 nM, 20 min, 37 °C). Mounted native specimens were examined and photographs were taken by an epi-fluorescent microscope Nikon Eclipse E 400 (Nikon, Prague, Czech Republic). Cytoplasms of at least 1000 cells were quantified with subsequent morphometric analysis using the software NIS Elements AR 3.20. Results were expressed as percentage of cells positive for superoxide radical production.

2.8. Mitochondrial membrane potential (MMP) analysis

Mitochondrial membrane potential analysis in 2.5 μmol selenite-exposed chemoresistant bladder cancer cells during 48 h was carried out using mitochondrial cationic JC-1 dye (10 μg/ml, 15 min, 37 °C) whose fluorescent emission color is potential-dependent: red – polarized mitochondrial membrane, green – depolarized mitochondrial membrane. Control and selenite-treated cells in cytospin chambers were mounted and changes in MMP in at least 1000 cells were assessed with an epifluorescence microscope Nikon Eclipse E 400 (Nikon, Prague, Czech Republic) (TRITC and FITC-specific filters). In obtained photographs mitochondria of at least 1000 cells were analyzed using the software NIS Elements AR 3.20. Results were expressed as percentage of cells with decreased mitochondrial membrane potential.

2.9. ATP production

ATP content in 2.5 μmol selenite-treated and control chemoresistant bladder cancer cells during 48 h was measured by ATP bioluminescent assay kit (Sigma-Aldrich, Cat. No. FLAA, Prague, Czech Republic) as recommended by manufacturer. Briefly, grown control and selenite-exposed cells were collected and lysed as described in Section 2.6. The lysates were resuspended in PBS and the amount of protein in supernatant was determined by BCA assay. Based on the amount of protein present in individual supernatant samples, these were then adjusted by dilution or concentration to insure that measured ATP would correspond to the equal number of cells in both controls and treated populations per given time interval. Chemoluminescent reaction of sample supernatants as well as blanks was then measured in glass vials and their final ATP content was calculated from calibration curves obtained by the same reaction with provided ATP standards. Results were expressed as a percentage of control.

2.10. Lysosomal permeabilization

To measure lysosomal membrane integrity in 2.5 μmol selenite-treated chemoresistant bladder cancer cells during 48 h, both control and treated cells in 96-well plates were washed in warm medium and at individual treatment intervals were stained with 5 μM AO for 15 min in an incubator. At the end of incubation, cells were rinsed twice with fresh cultivation medium and AO redistribution was measured with a SpectrafluorPlus (TECAN Austria GmbH, Grödig, Austria) at 490/530 nm wavelengths. An increase in diffuse cytosolic green fluorescence by AO released from lysosomes indicated loss of lysosomal membrane integrity [21].

2.11. Autophagy assays

2.11.1. Detection of autophagosomes

The rate of autophagy was measured in control and 2.5 μmol selenite-treated cells during 48 h by a detection of MDC-specific autophagic fluorescence. Briefly, cells grown in 96-well plates with transparent bottom were at individual time intervals incubated with 50 μM MDC in DMSO for 15 min at 37 °C at dark. After incubation, wells were thoroughly rinsed twice in PBS and MDC-positive fluorescence was quantified with a SpectrafluorPlus (TECAN Austria GmbH, Grödig, Austria) at 390/455 nm wavelength. Results are shown as fold increase in MDC-specific fluorescence relative to untreated cells.

2.11.2. Expression of autophagy proteins

The expression of autophagy markers BECLIN-1, p62 and LC3B in control and 2.5 μmol selenite-treated chemoresistant bladder cancer cells during 48 h was investigated using fluorescence microscopy and cytometric analysis. Cells were grown, treated and processed in 96-well plates as described in the Section 2.5. Primary anti-BECLIN-1 1:100; anti-p62 1:100 and anti-LC3B 1:100 and secondary Alexa Fluor 488 anti-mouse or anti-rabbit (1:250) antibodies were used. The fluorescence was analyzed by high-throughput cell scoring system with Cell scoring module of MetaXpress® Image Acquisition and Analysis Software.

2.12. Cell death analysis

2.12.1. Morphology and permeability assays

Cell death in chemoresistant bladder cancer cells treated with 2.5 μmol selenite during 48 h was determined by selective presence of cell morphology in combination with cell permeability method. Cells grown in tissue culture flasks or on coverslips were at individual treatment intervals analyzed morphologically or rinsed with warm medium (5 min) and stained with 0.5 μg/ml propidium iodide (PI) for 20 min (37 °C, dark). Thereafter, coverslips were mounted and the presence of PI in the cells along with their morphology were examined using a high-throughput cell scoring system with Cell scoring module of MetaXpress® Image Acquisition and Analysis Software. Together 3000 cells were examined.

2.12.2. Caspase-3 activity assay

Selenite (2.5 μmol)-treated and control chemoresistant bladder cancer cells grown in tissue culture flasks were at each treatment interval (0–48 h) harvested by centrifugation (1000 *g*, 5 min, JOUAN MR 22, Trigon, Prague, Czech Republic) and lysed on ice for 20 min in a lysis buffer (50 mM HEPES, 5 mM CHAPS and 5 mM DTT). The lysates were centrifuged at 14,000 *g*, 10 min, 4 °C and their enzyme activity was measured in a 96-well microplate using a kinetic fluorometric method based on the hydrolysis of the fluorogenic caspase-3-specific substrate (Ac-DEVD-AMC 37 °C, 1 h). Specific inhibitor of caspase-3 (Ac-DEVD-CHO) was used to confirm the specificity of the cleavage reaction. Fluorescence was recorded at 465/360 nm wavelength using a SpectraFluor Plus (TECAN Austria GmbH, Grödig, Austria).

2.12.3. Cell death typing

Damaged and dying cells were assorted to into three groups – apoptotic positive for blebbing morphologies, increased caspase-3 activity and the absence of PI staining, necrotic positive for cell ballooning or shrinkage, absent caspase-3 activity and the presence of PI staining and others showing a range of morphological changes often accompanied by vacuolization in the absence of caspase-3 activity and PI staining.

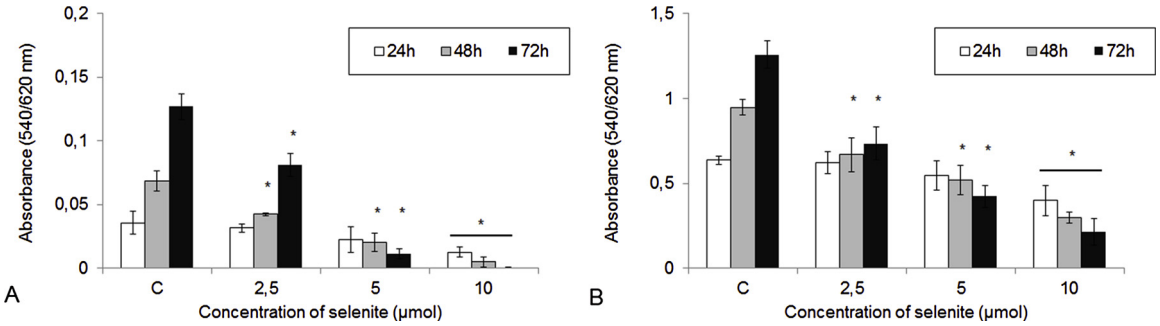

Fig. 1. Antiproliferative effects of sodium selenite (Na_2SeO_4 – selenite) on chemoresistant bladder cancer cells RT-112/D21. Cells were exposed to a range of selenite concentrations and cell growth and viability (up to 72 h) were measured by Neutral red and Brilliant blue assays as described in Materials and methods section. (A) Neutral red assay (B) Brilliant blue assay. Values represent means ± SD of at least three experiments *P < 0.05 compared to untreated control cells at the same treatment interval with one way-Anova test and Dunnett's post test for multiple comparisons (For interpretation of the references to colour in this figure legend, the reader is referred to the web version of this article).

2.13. Statistics

Data analysis was performed by GraphPad Prism (GraphPad Software version 6.0, Inc. San Diego, U.S.A.). Statistical analysis was carried out using one-way analysis of variance (ANOVA) followed by Dunnett's multiple comparisons test significant at a level of $P < 0.05$.

3. Results

3.1. Cytotoxic effects of selenite in chemoresistant bladder cancer cells RT-112/D21

Cytotoxic effects of selenite at a range of concentrations were evaluated during 72 h of exposure in chemoresistant bladder cancer cells RT-112/D21 using two established assays measuring cell viability via membrane integrity and cell growth via quantification of total protein content. Selenite-mediated inhibitory effects were concentration-dependent, with the lowest selenite concentration producing significant cytotoxicity during 48–72 h of treatment was 2.5 μmol whereas the significant cytotoxicity during 24 h of exposure was associated with the highest concentration tested (i.e. 10 μmol) only (Fig. 1A, B). These effects were further confirmed by time-lapse videomicroscopy based morphological observations (Fig. 2). They revealed rather significant differences in treated cells morphologies and behavior upon individual selenite treatment. The higher selenite concentrations produced early development of a heterogeneous cytoplasmic vacuolization in perinuclear area of exposed cells, their collective loss of adherence to substratum followed by overall collapse (shrinkage) or cell ballooning. On the other hand, upon low selenite exposure cells first did not show any major morphological perturbations other then occasional enlargement or clumping. Still, in comparison with control cultures their proliferation was almost stopped. At later treatment intervals (24 h and onward) selenite-exposed cells showed some vacuolization although less pervasively and gradually tended to round up and/or collapse individually in a longer time frame. With respect to the above-mentioned results we chose to continue testing the lowest efficient selenite concentration.

3.2. Low selenite induces antiproliferative signaling in chemoresistant bladder cancer cells RT-112/D21

In order to confirm the extent of molecular changes associated with an early selenite-dependent inhibition of proliferation, the expression of selected proliferation-specific proteins was evaluated using high content analysis. Our presented data demonstrate that in the spectrum of evaluated proteins and time interval 24 h of exposure to 2.5 μmol selenite, the expressions of cell cycle inhibitors p21 and p16 were significantly increased. This trend continued into 48 h of exposure interval and was accompanied by a significant decrease in AKT and ERK1/2 expressions (Fig. 3A). The drop in the expression of all the followed AKT forms was specifically visible with markedly decreasing ratio of phosphorylated to total protein: p-AKT1 to AKT1 0.85 at 24 h of exposure and 0.22 at 48 h of exposure; p-AKT2 to AKT2 0.75 at 24 h of exposure and 0.27 at 48 h of exposure and p-AKT3 to AKT3 0.85 at 24 h of exposure and 0.1 at 48 h of exposure (Fig. 3B). Conversely, the expressions of cyclin D1 (CYCD), c-MYC, p53 or PTEN were not changed significantly as well as the expression of p38 which remained at the same basal level during 48 h of treatment (Fig. 3A).

3.3. Cytotoxic selenite concentration is tolerated in normal urothelial cells UROtsa

In order to verify biological effects of the tested range of selenite concentrations in normal human cells, we carried out the same biochemical and morphological assays (see above) during 72 h in human urothelial UROtsa cells. As demonstrated in Fig. 4A, B, the highest selenite concentrations significantly reduced cell growth, proliferation and viability of exposed cultures at later treatment intervals of 48–72 h. On the other hand, the lowest selenite concentration of 2.5 μmol, which was chosen for further studies, had no adverse effect to all evaluated parameters in exposed cultures at all treatment intervals. In addition, time-lapse analyses of thus treated cells demonstrated very few changes in exposed cells both in terms of their morphology as well as behavior (Fig. 4C).

3.4. Low selenite induces superoxide production but does not damage DNA in chemoresistant bladder cancer cells RT-112/D21

Time course analysis of 2.5 μmol selenite-treated cells positive for superoxide anion revealed their significant increase firstly at the 24 h treatment interval with culmination at 36 h of exposure (Fig. 5B). Conversely, no significant DNA damage as measured by comet assay occurred at any treatment interval although a slight elevation occurred at later treatment intervals (Fig. 5A).

3.5. Low selenite interferes with mitochondria

Preliminary microscopic analyses of RT-112/D21 cells exposed to 2.5 μmol selenite indicated changes in mitochondrial network (data not shown). These changes along with increased production of superoxide radical following selenite exposure suggested mitochondria as a likely target of selenite-mediated toxicity. Accordingly, to 2.5 μmol selenite concentration reduced mitochondrial production of ATP as well as mitochondrial membrane potential (MMP) approximately in the same time frame (i.e. first significant decrease at 24 h of exposure) where superoxide production increased (Fig. 5C, D).

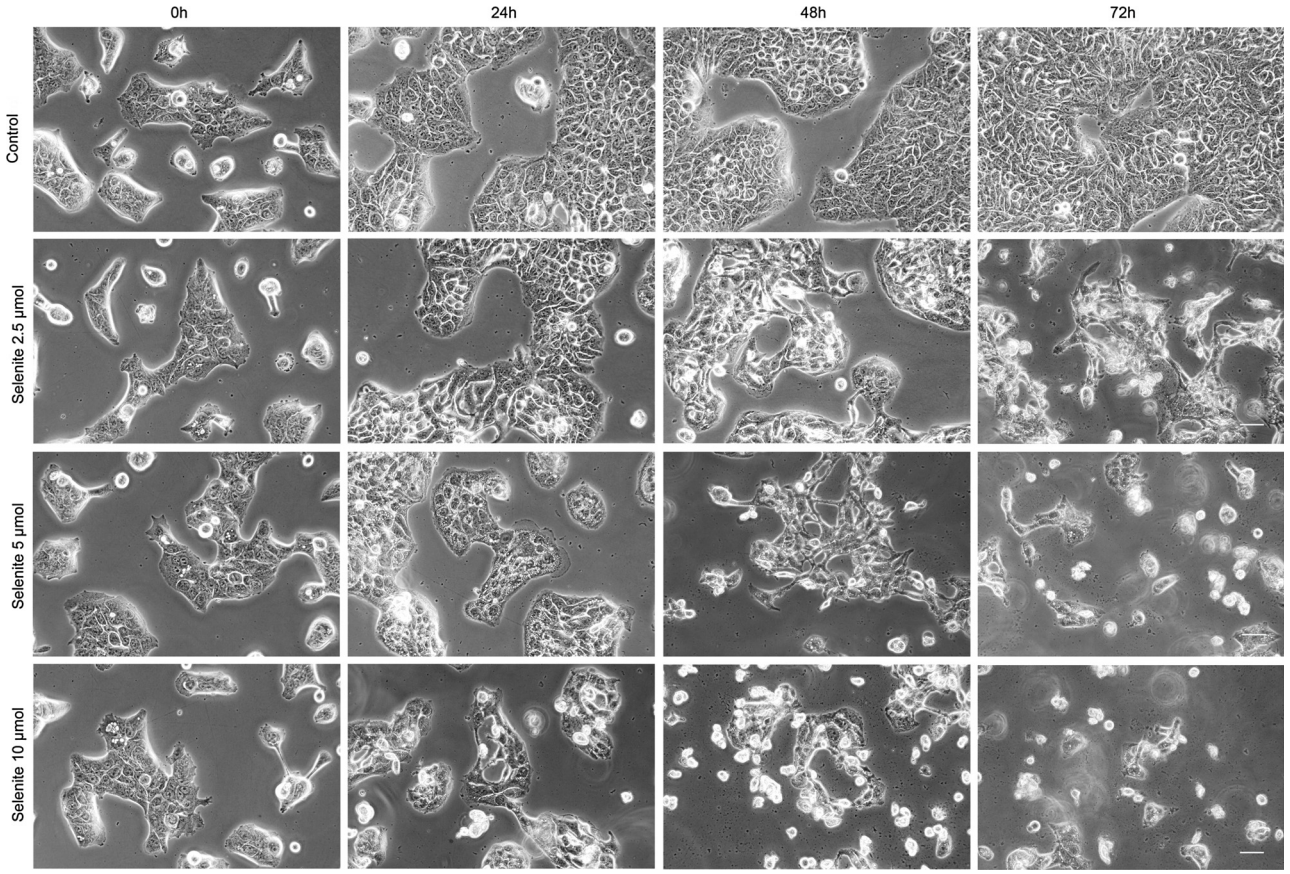

Fig. 2. Time-lapse videomicroscopy of chemoresistant bladder cancer cells RT-112/D21 exposed to a range of sodium selenite (Na_2SeO_4 – selenite) concentrations during 72 h. Control and selenite-exposed cultures were recorded using BioStation IM upon various time-lapse modes and magnifications. Presented are typical culture morphologies out of at least five independent experiments. Phase contrast 400 × . Bar 30 µm.

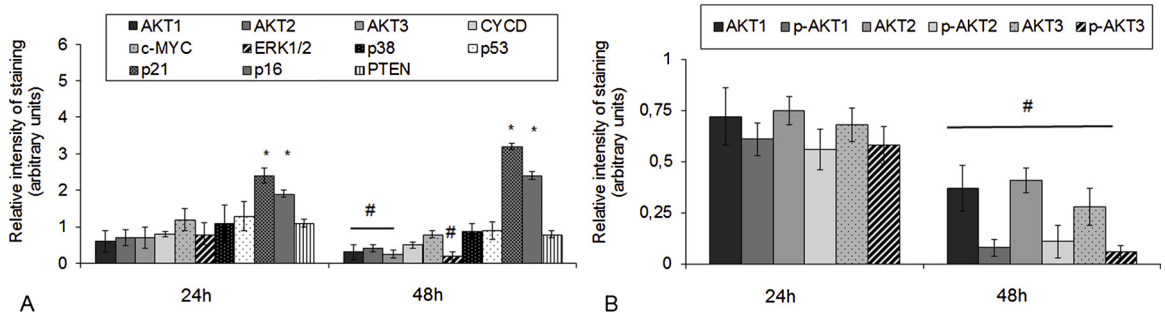

Fig. 3. Effect of 2.5 µmol sodium selenite (Na_2SeO_4 – selenite) on select proliferation markers expression in chemoresistant bladder cancer cells RT-112/D21 during 48 h. Cells were exposed to external selenite, fixed, permeabilized and after incubation with particular antibody; corresponding fluorescence was measured by the Cell Scoring module of MetaXpress® Image Acquisition and Analysis Software. (A) Expression of AKT1, AKT2, AKT3, CYCD, c-MYC, ERK1/2, p38, p53, p16, p21 and PTEN (B) Expression of AKT1, p-AKT1, AKT2, p-AKT2, AKT3, p-AKT3. Results represent means ± SD of at least three experiments. $P < 0.05$ * Significantly higher than control at the same treatment interval, (A) $P < 0.05$ # lower than control at the same treatment interval (B) $P < 0.05$ # lower than treated cells at 24 h of exposure with a one way-Anova test and Dunnett's post test for multiple comparisons.

3.6. Lysosomal membrane permeabilization (LMP) in low selenite exposed chemoresistant bladder cancer cells RT-112/D21

We used an assay which quantifies the extent of AO displacement from lysosomes to the cytoplasm. The results of this assay show that in 2.5 µmol selenite exposed bladder cancer cells the translocation of AO into cytoplasm occurred at late treatment intervals resulting in a significant elevation in free cytoplasmic AO content in the cells (Fig. 6).

3.7. Selenite activates autophagy in chemoresistant bladder cancer cells RT-112/D21

Due to the occurrence of vacuolar morphology in low selenite-exposed cells and with the relatively slow buildup of toxicity, the presence of autophagy and its involvement in selenite-dependent damaging was also investigated. Analyses of MDC-specific fluorescence, which is an indicative of autophagic presence in the system, proved its significant increase at 12 h of exposure and onwards (Fig. 7A). Moreover, dynamics of expression of other specific autophagy markers (i.e. LC3B, p62 and BECLIN-1) indicated an active autophagy process in treated

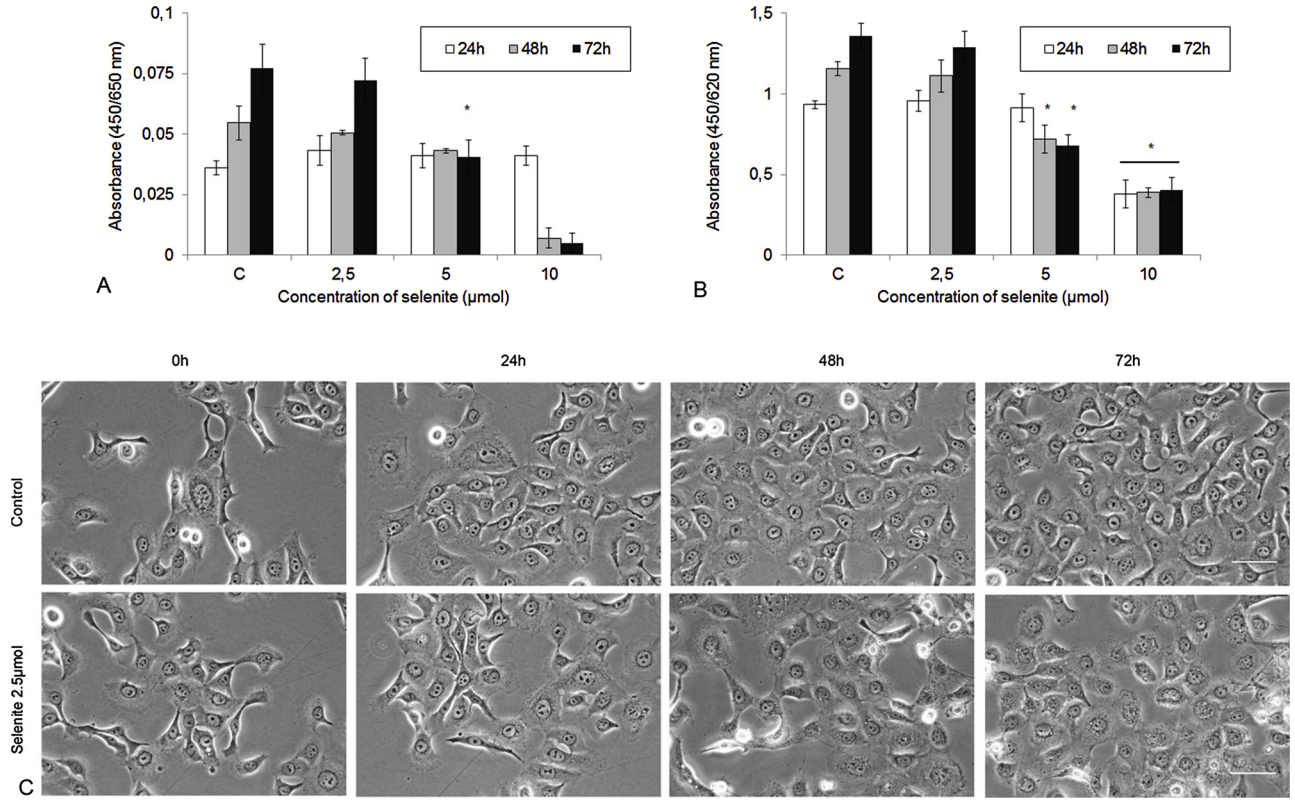

Fig. 4. Antiproliferative effects of sodium selenite (Na_2SeO_4 – selenite) on human urothelial cell line UROtsa. Cells were exposed to selenite and cell growth and viability (up to 72 h) were measured by several biochemical and morphological methods as described in Materials and methods section. (A) Neutral red assay (B) Brilliant blue assay (C) Time-lapse videomicroscopy. Values represent means ± SD of at least three experiments *P < 0.05 compared to untreated control cells at the same treatment interval with one way-Anova test and Dunnett's post test for multiple comparisons. Presented are typical culture morphologies out of at least five independent experiments. Phase contrast 400 × . Bar 30 µm (For interpretation of the references to colour in this figure legend, the reader is referred to the web version of this article).

cells (Fig. 7B).

3.8. Low selenite induced death in chemoresistant bladder cancer cells RT-112/D21 is phenotypically variable

Although delayed in time, 2.5 µmol selenite ultimately induced in exposed bladder cancer cultures cell death. RT-112/D21 cells presented variable morphological alterations including clustered or individual cell rounding, shrinkage and/or membrane blebbing (Figs. 2 and 8 A). Contrary to the caspase-3 activity which was not significantly increased during all treatment intervals (Fig. 8C), numbers of cells with the damaged membrane markedly increased already at 24 h of exposure and they continued to grow until 48 h of exposure (Fig. 8B). Less than 20% of treated cells were positive for necrosis and approximately 30% of treated cells showed a combination of cell death markers with no distinct and homogeneous cell death modality (Fig. 8D).

3.9. Various signaling pathways contribute to low selenite-dependent cell death in chemoresistant bladder cancer cells RT-112/D21

To mechanistically verify the involvement of several notorious death signals in the 2.5 µmol selenite-mediated activated cell demise, a series of chemical/pharmacological inhibitors blocking oxidative stress (NAC), autophagy (3-MA), caspases (z-VAD), aspartate activities (pepstatin A) and cytochrome c release (CsA) were used. Although none of them had any significant effect on cell death rate in untreated cells (Fig. 9A), in 2.5 µmol selenite-exposed cells they showed a differing efficacy. The strongest effect was observed in case of antioxidant NAC which reduced cell demise by more than 50% while helping the cells to maintain their intact morphology. Autophagy as well as aspartate inhibitors also markedly prevented cell death although to the lesser degree than in NAC with the similar protective effect on treated cells morphology. Conversely, neither pan-caspase inhibitor not mitochondrial cytochrome c release blocker proved to attenuate selenite-mediated cell death (Fig. 9A, B).

4. Discussion

The role of selenite in the inhibition of bladder cancer remains in many areas underexplored and even controversial. Several available clinical trials brought inconsistent findings [4,22,23] and experimentally there is only very limited evidence concerning the nature of selenite effects on bladder cancer cells. In the current work selenite activity in chemoresistant bladder cancer cell line RT-112/D21 was investigated. We found that despite its acquired chemoresistance to the mentioned drugs, RT-112/D21 cells retain their sensitivity towards selenite which upon low concentration of 2.5 µmol inhibited during 48 h of exposure their growth and proliferation. In thus exposed cells the later gradual development of limited cytoplasmic vacuolization and individual morphological shape changes resulting in cells rounding and collapsing were noted too. These observations suggested that dynamics of selenite activity in chemoresistant RT-112/D21 cells is in fact biphasic; i.e. first cytostatic and next cytotoxic. The presence of an early selenite-mediated cytostatic effect in exposed cells was further confirmed by a steadily increased expression of cell cycle inhibitors p16 and p21 and through a significant decrease in proliferation-stimulating AKT and ERK1/2 expressions. This increased sensitivity of chemoresistant bladder cancer cells to the used low selenite concentration likely originated from the combined and simultaneous changes in selenite-intracellular targets including mitochondria, antioxidant systems or

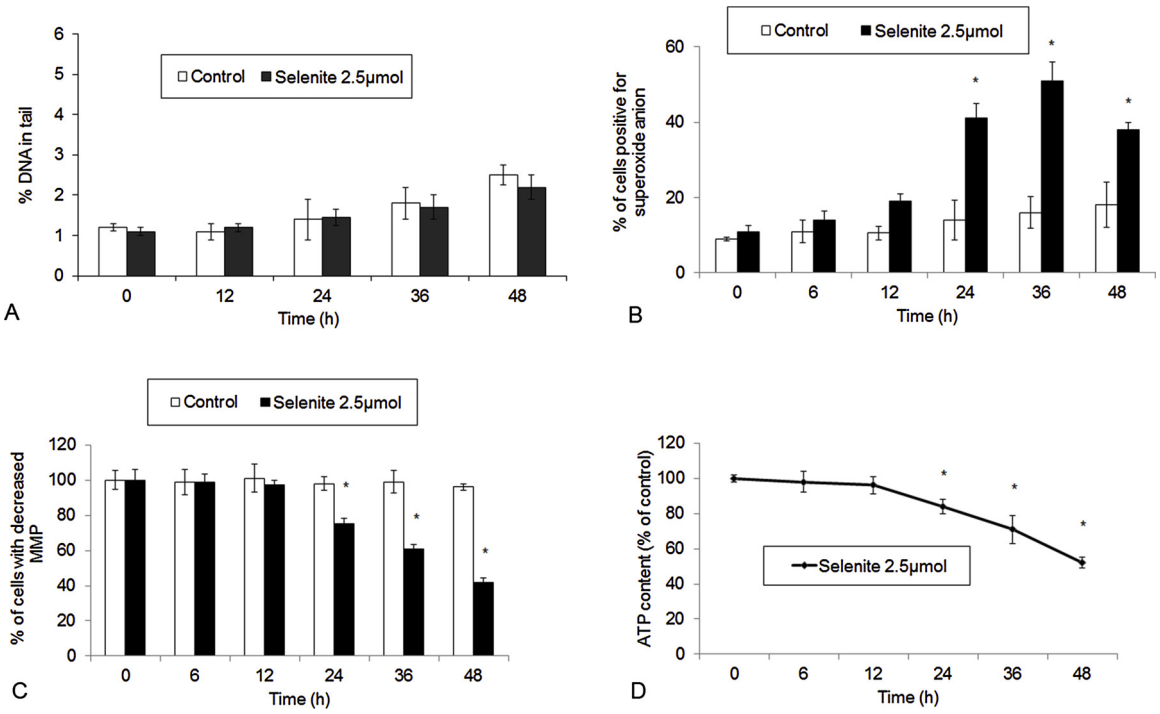

Fig. 5. Effects of 2.5 µmol sodium selenite (Na_2SeO_4 – selenite) on (A) DNA damage (B) superoxide production (C) mitochondrial membrane potential (MMP) and (D) ATP production in chemoresistant bladder cancer cells RT-112/D21 during 48 h. DNA damage was evaluated by comet assay, production of superoxide radicals was determined by MitoSOX™ Red reagent microscopically, MMP was determined by microscopic measurement of potential-sensitive JC-1 dye and ATP was determined bioluminescently as described in Materials and methods section. Values represent means ± SD of at least three experiments *P < 0.05 compared to untreated control cells at the same treatment interval with one way-Anova test and Dunnett's post test for multiple comparisons (For interpretation of the references to colour in this figure legend, the reader is referred to the web version of this article).

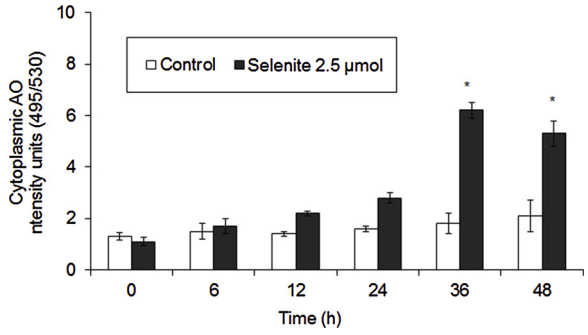

Fig. 6. Effect of 2.5 µmol sodium selenite (Na_2SeO_4 – selenite) on lysosomal membrane disruption in chemoresistant bladder cancer cells RT-112/D21 during 48 h. Lysosomal membrane integrity was quantitated via colorimetric determination of acridine orange (AO) translocation from lysosomes into the cytoplasm as described in Materials and methods section. Results represent means ± SD of at least three experiments *P < 0.05 compared to untreated control cells at the same time interval with one way-Anova test and Dunnett's post test for multiple comparisons.

individual proteins as discussed below. Equally important for this cytotoxicity could be the effect of extracellular environment and, in particular extracellular reduction mediated by cysteine. The export of cysteine residues via multidrug resistance proteins in tumor cells is acknowledged, leading to the increased production of selenide with elevated selenite toxicity in the close proximity of chemoresistant cells [24]. In addition, duration of selenite exposure was an important factor too as indicated by our observed time-dependent biphasic selenite effect. Which of the proposed mechanisms was chiefly responsible for the observed sensitivity of the tested cells to selenite in this context cannot be fully determined and certainly deserves further mechanistic exploration. On the other hand, and quite importantly, none of these findings were present in selenite-treated normal urothelial cells UROtsa which corresponds to the known and acknowledged selectivity of selenite in tumor versus normal cells [11,24].

In this respect, mitochondria have been acknowledged to be an important target of selenite toxicity and a major producer of superoxide radical responsible for damaging of DNA as well as other macromolecules or organelles [15,25–27]. In our experimental model, selenite induced a rather early marked increase in superoxide anion levels which were accompanied by predictable loss of mitochondrial membrane potential as well as by decreasing ATP production. On the other hand, no significant DNA damage was recorded in our cells unlike previously published evidence [28,29]. The most likely explanation of this discrepancy is the employed selenite concentration-related extent and timing of ROS levels generation in exposed cells since higher selenite doses do markedly alter DNA and stimulate relevant cell stress response as shown by us previously [30].

Increased levels of ROS may generate oxidative stress which cells attempt to combat using various defense mechanisms including autophagy. Autophagy is a dynamic process involving multi-step formation of autophagosomes and their lysosomal degradation under control of autophagy-related genes [31]. Since selenite has been known to influence autophagy in several types of tumor cells [32,33] we have investigated its presence using several standard markers. Our data show an early and fast elevation of MDC-specific fluorescence in treated cells, indicative of enhanced production of autophagosomes due to increased autophagy which was also confirmed by increasing protein abundance of BECLIN-1 and LC3B as well as by decreasing amount of p62. Besides its effect on autophagy, selenite exposure adversely affected the integrity of lysosomes and induced lysosomal membrane permeability (LMP) with subsequent proteases-mediated activation of cell death [34]. LMP is known to occur as a result of oxidative stress which seems to be the case here as our employed antioxidant NAC reduced LMP (data not shown). Moreover, the existence of damaged lysosomes

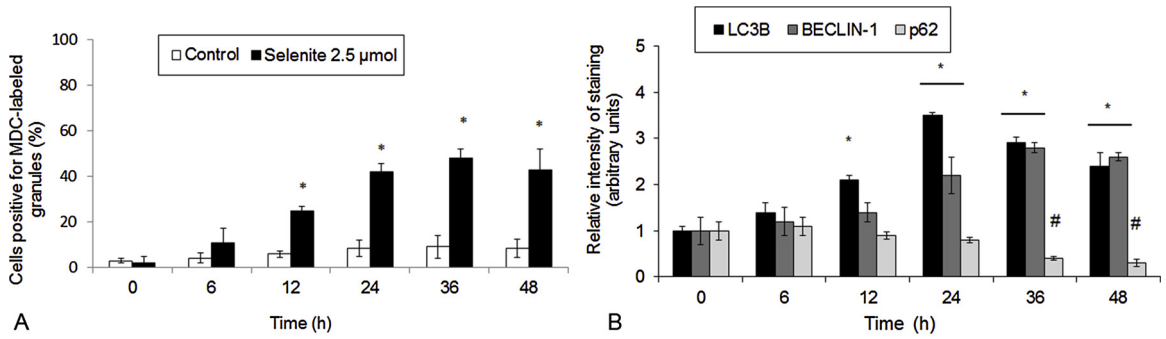

Fig. 7. Autophagy in chemoresistant bladder cancer cells RT-112/D21 exposed to 2.5 µmol sodium selenite (Na_2SeO_4 – selenite) as measured by (A) MDC-positive granules and (B) protein expression of selected autophagy-related proteins LC3B, p62 and BECLIN-1 during 48 h as described in Materials and methods section. Values represent means ± SD of at least three experiments (A) *P < 0.05 compared to the untreated cells at the same treatment interval (B) *P < 0.05 and #P < 0.05 compared to the beginning of treatment with one way-Anova test and Dunnett's post test for multiple comparisons.

unable to fuse with arising autophagosomes further corroborates their observed accumulation in selenite-treated cells contributing to the overall increase in autophagy.

Selenite-dependent acute or chronic damaging of cells finally results in phenotypically pleiotropic cell death comprising classical caspase-dependent apoptosis [35], caspase-independent apoptosis [36] or necrosis [37]. Moreover, autophagic or mitophagic cell death as well as programmed necrosis represent other cell death modalities reported in tumor cells exposed to selenite [13,38,39].

Cell death in the tested bladder cancer cells treated with selenite was detectable from 24 h of treatment and presented several phenotypes. The morphology of exposed cells varied significantly, with same cells displaying features of classical apoptosis (i.e. rounding, blebbing, shrinkage) while others showing necrotic morphology (i.e. enlargement, rupture and fragmentation) and majority being in a continuum between the above mentioned extremes. Subsequent assays into membrane permeability and caspase-3 activity confirmed the growing presence of the former but the absence of later in the studied cells. Such heterogeneity is perhaps surprising, and particularly in the light of other published evidence which typically reports seemingly homogeneous behavior of treated cells [13,40] but it is logical since treated populations are not synchronized and would likely respond individually to the given exposure. Moreover, the use of several complementary techniques along with focus on individual cells often reveals qualitative differences among the cells which would go otherwise unnoticed.

In order to mechanistically verify the involvement of various selenite-dependent mechanisms in the final cell death extent, several chemical inhibitors were used. Despite of the fact that none of them was able to completely prevent selenite-induced cell death, several of them; i.e. autophagy inhibitor 3-MA, antioxidant NAC and aspartate inhibitor pepstatin A significantly reduced it. Conversely, pan-caspase inhibitor as well cytochrome c release inhibitor showed no effect. These results clearly suggest that selenite-mediated inhibitory effects are in the employed bladder cancer cells multifaceted and occur via oxidative stress-

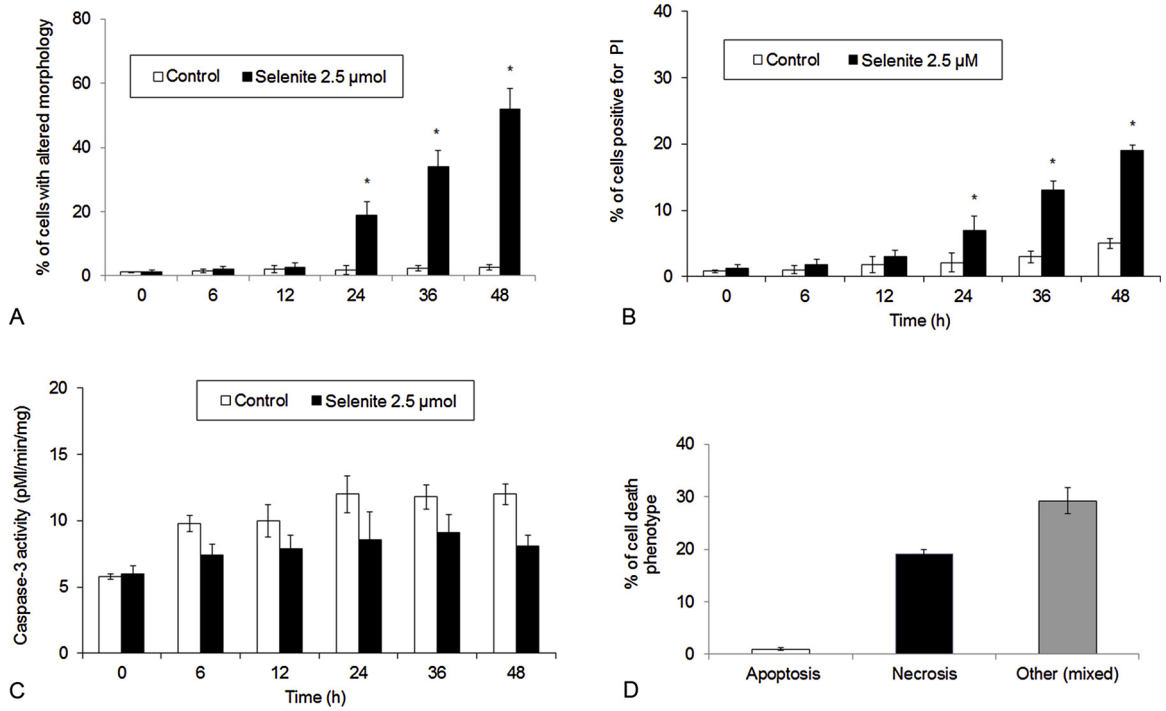

Fig. 8. Cell death and its phenotypes in chemoresistant bladder cancer cells RT-112/D21 exposed to 2.5 µmol sodium selenite (Na_2SeO_4 – selenite) as measured by (A) cellular morphology (B) propidium iodide (PI) permeability and (C) caspase-3 activity with (D) final cell death phenotype groupings during 48 h. Cells were exposed to selenite and individual parameters were measured as described in Materials and methods section. Distribution of dead cells into respective phenotypic groups was based on the presence of the above mentioned features. Values represent means ± SD of at least three experiments *P < 0.05 compared to the untreated controls at the same time interval with one way-Anova test and Dunnett's post test for multiple comparisons.

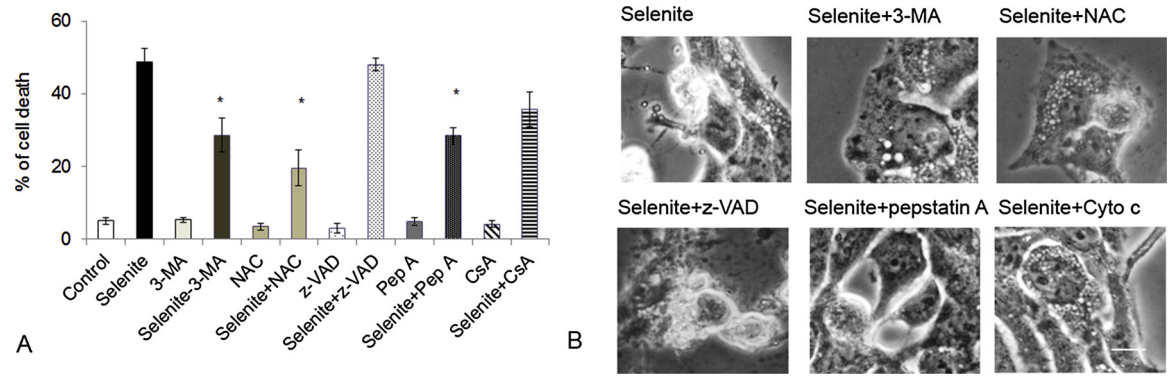

Fig. 9. The effects of various chemical inhibitors on 2.5 µmol sodium selenite (Na_2SeO_4 – selenite)-induced cell death in chemoresistant bladder cancer cells RT-112/D21 during 48 h of exposure. Inhibitors of oxidative stress (N-acetylcystein (NAC)), caspases (z-VAD), autophagy (3-methyladenine (3-MA)), aspartic acid proteases (pepstatin A (Pep A)) and cytochrome c mitochondrial release (cyclosporine A (CsA)) were firstly supplied to the cells without selenite and then prior to or simultaneously with selenite and the extent of cell death was determined as described in Materials and methods section. (A) Cell death extent after inhibitors alone, selenite and selenite with individual inhibitors at 48 h of exposure (B) morphological appearance of cells after selenite with individual inhibitors at 48 h of exposure. Values represent means ± SD of at least three experiments *P < 0.05 compared to the Se-exposed cells at the same time interval with one way-Anova test and Dunnett's post test for multiple comparisons. Presented are typical culture morphologies out of at least five independent experiments. Phase contrast 400 × . Bar 5 µm.

dependent suppression of proliferative signaling, activation of autophagy, damage of mitochondria and lysosomes and stimulation of heterogeneous cell death where classical caspase-dependent pathways are not involved.

5. Conclusion

It is demonstrated that selenite upon low concentration of 2.5 µmol produces first cytostatic and then cytotoxic effects in chemoresistant bladder cancer cells RT-112/D21. Selenite via oxidative stress suppresses proliferative signaling, damages mitochondria and lysosomes and induces cell death comprising necrotic, apoptotic and autophagic phenotypes. These adverse selenite-dependent changes are not observed in normal urothelial cells which constitutes the basis for further testing of this compound in preclinical and clinical models. These should firstly take into consideration some aspects of selenite toxicity in bladder cancer cells which were not addressed in the present study. It is among others the diffusion of the given selenite concentration (dose) to the tumor in vivo, its efficacy in terms of stimulation of oxidative stress in often hypoxic cancer cells as well as their chemoresistance and thus responsiveness to selenite which might differ upon their grade.

Declaration of interest

None.

Acknowledgment

This work was supported by the program PROGRES Q40/1.

References

[1] L.V. Papp, A. Holmgren, K.K. Khanna, Selenium and selenoproteins in health and disease, Antioxid. Redox Signal. 12 (7) (2010) 793–795.
[2] M.P. Rayman, Selenium and human health, Lancet 379 (9822) (2012) 1256–1268.
[3] G. Combs Jr., W. Gray, Chemopreventive agents: selenium, Pharmacol. Ther. 79 (3) (1998) 179–192.
[4] E. Kellen, M. Zeegers, F. Buntinx, Selenium is inversely associated with bladder cancer risk: a report from the Belgian case-control study on bladder cancer, Int. J. Urol. 13 (9) (2006) 1180–1184.
[5] M.A. Knowles, C.D. Hurst, Molecular biology of bladder cancer: new insights into pathogenesis and clinical diversity, Nature Rev Cancer 15 (1) (2015) 25–41.
[6] M.S. Soloway, Bladder cancer: Lack of progress in bladder cancer–what are the obstacles? Natur Rev Urol. 10 (1) (2013) 5–6.
[7] M. Brinkman, F. Buntinx, E. Muls, M.P. Zeegers, Use of selenium in chemoprevention of bladder cancer, Lancet Oncol. 7 (9) (2006) 766–774.
[8] C. Ip, C. Hayes, R.M. Budnick, H.E. Ganther, Chemical form of selenium, critical metabolites, and Cancer prevention, Cancer Res. 51 (2) (1991) 595–600.
[9] E.N. Drake, Cancer chemoprevention: selenium as a prooxidant, not an antioxidant, Med. Hypotheses 67 (2) (2006) 318–322.
[10] M. Vinceti, T. Filippini, C. Del Giovane, G. Dennert, M. Zwahlen, M. Brinkman, M.P. Zeegers, M. Horneber, R. D'Amico, C.M. Crespi, Selenium for preventing cancer, Cochrane Database Syst. Rev. 1 (2018) CD005195.
[11] G. Nilsonne, E. Olm, A. Szulkin, F. Mundt, A. Stein, B. Kocic, A.K. Rundlof, A.P. Fernandes, M. Bjornstedt, K. Dobra, Phenotype-dependent apoptosis signalling in mesothelioma cells after selenite exposure, J Exp Clin Cancer Res: CR 28 (2009) 92.
[12] J.E. Spallholz, On the nature of selenium toxicity and carcinostatic activity, Free Radic. Biol. Med. 17 (1) (1994) 45–64.
[13] M. Wallenberg, S. Misra, A.M. Wasik, C. Marzano, M. Bjornstedt, V. Gandin, A.P. Fernandes, Selenium induces a multi-targeted cell death process in addition to ROS formation, J. Cell. Mol. Med. 18 (4) (2014) 671–684.
[14] F. Huang, C. Nie, Y. Yang, W. Yue, Y. Ren, Y. Shang, X. Wang, H. Jin, C. Xu, Q. Chen, Selenite induces redox-dependent Bax activation and apoptosis in colorectal cancer cells, Free Radic. Biol. Med. 46 (8) (2009) 1186–1196.
[15] E.H. Kim, K.S. Choi, A critical role of superoxide anion in selenite-induced mitophagic cell death, Autophagy 4 (1) (2008) 76–78.
[16] J.J. Marin, O. Briz, M.J. Monte, A.G. Blazquez, R.I. Macias, Genetic variants in genes involved in mechanisms of chemoresistance to anticancer drugs, Curr. Cancer Drug Targets 12 (4) (2012) 402–438.
[17] S.T. Pan, Z.L. Li, Z.X. He, J.X. Qiu, S.F. Zhou, Molecular mechanisms for tumour resistance to chemotherapy, Clin. Exp. Pharmacol. Physiol. Suppl. 43 (8) (2016) 723–737.
[18] S. Misra, M. Boylan, A. Selvam, J.E. Spallholz, M. Bjornstedt, Redox-active selenium compounds–from toxicity and cell death to cancer treatment, Nutrients 7 (5) (2015) 3536–3556.
[19] N. Hail Jr., M. Cortes, E.N. Drake, J.E. Spallholz, Cancer chemoprevention: a radical perspective, Free Radic. Biol. Med. 45 (2) (2008) 97–110.
[20] O. Seemann, M. Muscheck, M. Siegsmund, H. Pilch, C.T. Nebe, J. Rassweiler, P. Alken, Establishment and characterization of a multidrug-resistant human bladder carcinoma cell line RT112/D21, Urol. Res. 22 (6) (1995) 353–360.
[21] J. Pourahmad, S. Ross, P.J. O´Brien, Lysosomal involvement in hepatocyte cytotoxicity induced by Cu(2+) but not Cd(2+), Free Radic. Biol. Med. 30 (1) (2001) 89–97.
[22] R. Muecke, L. Schomburg, J. Buentzel, K. Kisters, O. Micke, E. German Working Group Trace, O, Electrolytes in, Selenium or no selenium–that is the question in tumor patients: a new controversy, Integr. Cancer Ther. 9 (2) (2010) 136–141.
[23] M.E. Goossens, M.P. Zeegers, H. van Poppel, S. Joniau, K. Ackaert, F. Ameye, I. Billiet, J. Braeckman, A. Breugelmans, J. Darras, K. Dilen, L. Goeman, B. Tombal, S. Van Bruwaene, B. Van Cleyenbreugel, F. Van der Aa, K. Vekemans, F. Buntinx, Phase III randomised chemoprevention study with selenium on the recurrence of non-invasive urothelial carcinoma. The SELEnium and BLAdder cancer Trial, Eur. J. Cancer 69 (2016) 9–18.
[24] E. Olm, A.P. Fernandes, C. Hebert, A.K. Rundlof, E.H. Larsen, O. Danielsson, M. Bjornstedt, Extracellular thiol-assisted selenium uptake dependent on the x(c)-cystine transporter explains the cancer-specific cytotoxicity of selenite, Proc. Natl. Acad. Sci. U.S.A. 106 (27) (2009) 11400–11405.
[25] H.T. Wang, X.L. Yang, Z.H. Zhang, J.L. Lu, H.B. Xu, Reactive oxygen species from mitochondria mediate SW480 cells apoptosis induced by Na2SeO3, Biol. Trace Elem. Res. 85 (3) (2002) 241–254.
[26] W. Zhong, T.D. Oberley, Redox-mediated effects of selenium on apoptosis and cell cycle in the LNCaP human prostate cancer cell line, Cancer Res. 61 (19) (2001)

7071–7078.
[27] Y. Zhu, H. Xu, K. Huang, Mitochondrial permeability transition and cytochrome c release induced by selenite, J. Inorg. Biochem. 90 (1-2) (2002) 43–50.
[28] L. Letavayova, V. Vlckova, J. Brozmanova, Selenium: from cancer prevention to DNA damage, Toxicology 227 (1-2) (2006) 1–14.
[29] R.A. Yu, C.F. Yang, X.M. Chen, DNA damage, apoptosis and C-myc, C-fos, and C-jun overexpression induced by selenium in rat hepatocytes, Biomed. Environ. Sci. 19 (3) (2006) 197–204.
[30] K. Rezacova, K. Canova, A. Bezrouk, E. Rudolf, Selenite induces DNA damage and specific mitochondrial degeneration in human bladder cancer cells, Toxicol. In Vitro 32 (2016) 105–114.
[31] I. Dikic, Z. Elazar, Mechanism and medical implications of mammalian autophagy, Nature Rev. Mol Cell Biol. 19 (6) (2018) 349–364.
[32] Q. Jiang, F. Li, K. Shi, Y. Yang, C. Xu, Sodium selenite-induced activation of DAPK promotes autophagy in human leukemia HL60 cells, BMB reports 45(3) (2012) 194–199.
[33] S.H. Park, J.H. Kim, G.Y. Chi, G.Y. Kim, Y.C. Chang, S.K. Moon, S.W. Nam, W.J. Kim, Y.H. Yoo, Y.H. Choi, Induction of apoptosis and autophagy by sodium selenite in A549 human lung carcinoma cells through generation of reactive oxygen species, Toxicol. Lett. 212 (3) (2012) 252–261.
[34] M.E. Guicciardi, M. Leist, G.J. Gores, Lysosomes in cell death, Oncogene 23 (16) (2004) 2881–2890.
[35] C. Jiang, H. Hu, B. Malewicz, Z. Wang, J. Lu, Selenite-induced p53 Ser-15 phosphorylation and caspase-mediated apoptosis in LNCaP human prostate cancer cells, Mol. Cancer Ther. 3 (7) (2004) 877–884.
[36] K. Jonsson-Videsater, L. Bjorkhem-Bergman, A. Hossain, A. Soderberg, L. Eriksson, C. Paul, A. Rosen, M. Bjornstedt, Selenite-induced apoptosis in doxorubicin-resistant cells and effects on the thioredoxin system, Bioch Pharmacol. 67 (3) (2004) 513–522.
[37] M. Freitas, V. Alves, A.B. Sarmento-Ribeiro, A. Mota-Pinto, Combined effect of sodium selenite and docetaxel on PC3 metastatic prostate cancer cell line, Biochem Biophys Res Comm. 408 (4) (2011) 713–719.
[38] J. Li, W. Qi, G. Chen, D. Feng, J. Liu, B. Ma, C. Zhou, C. Mu, W. Zhang, Q. Chen, Y. Zhu, Mitochondrial outer-membrane E3 ligase MUL1 ubiquitinates ULK1 and regulates selenite-induced mitophagy, Autophagy 11 (8) (2015) 1216–1229.
[39] C. Sanmartin, D. Plano, A.K. Sharma, J.A. Palop, Selenium compounds, apoptosis and other types of cell death: an overview for cancer therapy, Int. J. Mol. Sci. 13 (8) (2012) 9649–9672.
[40] H. Inoue, K. Tani, Multimodal immunogenic cancer cell death as a consequence of anticancer cytotoxic treatments, Cell Death Differ. 21 (1) (2014) 39–49.